# Structural Study and Properties of the Alkali Metal, Nitrosyl, and Ammonium Hepta- and Octafluorouranates(VI)

R. BOUGON,* P. CHARPIN, J. P. DESMOULIN, and J. G. MALM[1]

The thermal decomposition of the heptafluorouranates(VI) of the alkali metals is shown to take place in two steps. The first step gives the octafluorouranates(VI) and $UF_6$, and the decomposition rate is noticeable at temperatures above 100, 130, 150, and 210 °C for the Na, K, Rb, and Cs salts, respectively. The second step for $Na_2UF_8$ yields pure NaF and $UF_6$ above 300 °C, whereas the decomposition temperatures for the K, Rb, and Cs salts are above 300, 350, and 400 °C, respectively. Depending on the decomposition conditions, $F_2$ and $M_2UF_7$ (M = K, Rb, Cs) or $F_2$, $UF_6$, and $M_3UF_8$ are formed. The heptafluorouranates(VI) of all the cations studied, except for ammonium, were shown to exhibit dimorphism. The parameters of their cubic form were obtained and are as follows: $KUF_7$; $a = 5.22$ Å; $RbUF_7$; $a = 5.385$ Å; $CsUF_7$; $a = 5.517$ Å; $NOUF_7$; $a = 5.334$ Å; $NH_4UF_7$; $a = 5.393$ Å; $NaUF_7$(fccub), $a = 8.511$ Å, $Z = 4$. The x-ray pattern of the low-symmetry form of $CsUF_7$ just below the solid transition temperature (15 ± 1 °C) was indexed with a tetragonal cell where $a = 5.50$ Å and $c = 5.37$ Å. The x-ray diagrams of the low symmetry form of the other $MUF_7$ salts were not indexed, whereas those of the octafluorouranates were indexed with orthorhombic cells. The vibrational spectra of the hepta- and octafluorouranates were found to be very dependent on the temperature, and for the same temperature on the cation size. In the solids at high temperature the disordered F positions are likely to be averaged to give pseudo-$D_{5h}$ and $O_h$ symmetry structures for the $UF_7^-$ and $UF_8^{2-}$ ions, respectively. At lower temperature, as the motions are frozen out, the observed spectra for the hepta- and octafluorouranates arise from structures of symmetry no higher than $C_{2v}$ and $D_{2d}$, respectively. The ions $UF_7^-$ and $UF_8^{2-}$ were characterized in nitrosyl or cesium fluoride HF solutions, which were found to exchange $F^-$ ions with these anions. Based on observation of the chemical exchange between $UF_6$ and $UF_7^-$ and on a comparative study of the $WF_7^-$ ion, a fluoride ion transfer mechanism is also found for $UF_7^-$ dissolved in acetonitrile. Some trends observed in this study, like the thermal decomposition temperatures or the relative symmetries, are thought to arise from the differences in the cation–anion interaction. This interaction is stronger with smaller cations, which results in more distorted anions, less ionic U–F bonds, and paradoxically less stable complexes.

## Introduction

The syntheses and/or properties of hepta- and octafluorouranates(VI) have been described by several authors.[2-28] In a previous paper, in which the results of a study of the CsF and $NOF/UF_6$ systems were reported,[27] it was claimed, mainly from vibrational data, that the heptafluoro and octafluoro anions $UF_7^-$ and $UF_8^{2-}$ could have, at least in the solid state, a structure derived from a slight distortion of the idealized bipyramidal ($D_{5h}$) and cubic ($O_h$) structures, respectively. In a simultaneous paper,[28] in which x-ray and neutron diffraction work on $NOUF_7$ was reported, it was said that the diffraction patterns could just as well be representative of a monocapped octahedron provided that a statistical occupation of the seventh fluorine atom in the $x'x'x'$ sites was considered. To clear up this apparent discrepancy, a more extensive study was done on this subject in order to obtain a better idea of the structures of the $UF_7^-$ and $UF_8^{2-}$ ions. Some of the corresponding salts were studied both as solids and in solution, using vibrational spectroscopy, x-ray diffraction, and $^{19}F$ NMR spectroscopy. In addition to the data obtained on the anions themselves or their corresponding alkali metal or nitrosyl salts (such as solid–solid transitions or crystalline structures), some conclusions regarding the effect of the counterion on properties of these salts are given.

## Experimental Section

**Materials.** The compounds $UF_6$, $WF_6$, $F_2$, and HF were purchased from Comurhex; $UF_6$ was purified from HF by pumping at dry ice temperature; HF was treated with fluorine before use; and $F_2$ was used without purification. The alkali metal fluorides were purchased from Prolabo and dried either by melting in a crucible followed by cooling in a dry atmosphere or by degassing at 250 °C. $NH_4F$ purchased from Prolabo was used without purification. NOF was produced by first condensing NO, purchased from "l'Air Liquide", and $F_2$ together at liquid nitrogen temperature in a Monel reactor and then allowing the vessel to warm up to room temperature. In a similar manner, except in Kel-F reactors, the binary mixtures of CsF or NOF with anhydrous HF were obtained by condensing HF onto CsF or NOF. Acetonitrile or $SO_2$, purchased from Prolabo, was stored over $P_2O_5$ and introduced onto the sample by vaporization and condensation. Prior to use, propylene carbonate (4-methyl-2-dioxolone, $C_4H_6O_3$), purchased from Koch-Light Laboratories, was stored over 5 Å molecular sieves from Union Carbide International Co., and poured directly onto the sample in the drybox.

**Apparatus.** The volatile materials were transferred in a vacuum line made for the most part of Monel Metal tubing equipped with valves purchased from F. W. Co. and with differential gauges from "Etudes et Constructions Aéronautiques". For reactors, depending on the experimental requirements, glass bulbs, Kel-F tubes, Monel cylinders, or high-pressure vessels were used, these vessels being attached to the vacuum line through Monel, Kel-F, or Autoclave Engineer high pressure Monel valves. The nonvolatile solid samples were transferred in a drybox containing $P_2O_5$ as a desiccant.

**X-Ray Diffraction Patterns.** The Debye–Scherrer powder patterns were taken using a 114-mm diameter Philips instrument with copper $K\alpha$ radiation (1.5418 Å). The samples were contained in quartz capillaries ($\sim 0.5$ mm) and studies in the temperature range +40 to $-180$ °C were made possible by use of a Meric cryostat.

**Spectra.** Infrared spectra were recorded with a Beckman Model IR 9 and a Perkin-Elmer Model 457 in the ranges 4000–400 and 4000–250 cm$^{-1}$, respectively.

A few measurements were also made in the far-infrared region (400–40 cm$^{-1}$) using an FS 720 spectrophotometer. Powders were pressed between two thin plates of AgCl 12 mm in diameter or as a Nujol mull between plates of KBr or polyethylene disks. Solutions were studied using Barnes polyethylene molded cells (path length 0.2 mm). These cells were filled in the drybox with a Teflon syringe. The Raman spectra were recorded with a Coderg Model T 800 using the 514.5 nm line of a Model 165 Spectra Physics laser as the exciting light. For these spectra, the neat powders were contained in glass capillaries ($\sim 2$ mm) whereas the solutions were contained in KelF or FEP Teflon tubing (6 mm i.d.). The low-temperature spectra were obtained either with an Air Liquide cryostat for the liquid helium temperature range or a Coderg cryostat for temperatures above liquid nitrogen, in which cases the solid samples were contained in 30 cm long, 4 mm o.d., glass tubes or 8 mm long, $\sim 2$ mm o.d. capillaries, respectively. The frequency accuracy was estimated to be approximately ±3 cm$^{-1}$ for the infrared spectra and ±1 cm$^{-1}$ for the Raman spectra. The visible and near infrared spectra which were used for a further identification of the residues from the thermal decomposition of the octafluorouranates were recorded on a Cary 14 instrument. The corresponding powders were studied as Nujol mulls between two $CaF_2$ plates.

The ^{19}F NMR spectra were obtained on a Varian NV 14 spectrometer operating at 56.4 MHz equipped with a variable temperature probe and an extended scale allowing observation to be made as far as −675 ppm downfield from the $CFCl_3$ resonance. Furthermore, a Schlumberger frequency generator was used to shift the frequency scale even further so that the scale was extended to −953 ppm. The resonance frequencies were determined with a Schlumberger frequency counter. $CFCl_3$ was used as an external reference and the spectrometer was locked on this resonance. For these spectra the solutions were contained in a 6 mm o.d. Kel-F tube hot-pinched and placed into a 8 mm o.d. calibrated NMR tube containing a small amount of $CFCl_3$. The chemical shift accuracy was estimated to be ±0.1 ppm.

**Preparations.** The complexes $NOUF_7$ and $(NO)_2UF_8$ were prepared according to the methods previously described.[27] That is, $UF_6$ was reacted with a large excess of liquid NOF to get $(NO)_2UF_8$; $NOUF_7$ was obtained by reaction between stoichiometric amounts of NOF and $UF_6$ at dry ice temperature. The alkali metal fluoride–$UF_6$ complexes were also prepared as previously described[27] for $CsUF_7$ and $Cs_2UF_8$. That is, an excess of liquid $UF_6$ was reacted with the alkali metal fluorides to prepare the heptafluorouranates; controlled thermal decomposition of the $MUF_7$ salts (M = Na, K, Rb, Cs) under pumping yielded the octafluorouranates. To obtain the pure heptafluorouranates, however, it was found necessary to grind the mixture several times during the synthesis; after the $MF$–$UF_6$ mixture has been left at the chosen temperature for several hours, the excess $UF_6$ was pumped off at room temperature and the solid residue was ground in the dry box and then reacted further with $UF_6$. This procedure was repeated until pure $MUF_7$, as checked by its Raman spectrum, was obtained.

As already reported[19,21,27] the formation of the octafluorouranates is favored at high temperature, so for all the syntheses, the temperature was kept in the range 65–100 °C. It was found that under pumping the temperature at which decomposition of the heptafluorouranates was noticeable was 100, 130, 150, and 210 °C for the Na, K, Rb, and Cs salts, respectively. The $NH_4UF_7$ complex[10] was prepared by reaction between an excess of gaseous $UF_6$ and $NH_4F$ at room temperature, whereas $(NH_4)_2UF_8$ was obtained by using only the stoichiometric amount of $UF_6$. For some of the experiments performed with an excess of $UF_6$, a fast decomposition with the production of $NH_4UF_6$ spontaneously took place and consequently the decompositions of the ammonium salts were not studied. The decompositions of the alkali metal salts were studied either with an MCB Arion microcalorimeter connected to a homemade microsublimation–microdesorption apparatus, or a Monel reactor connected to the vacuum line.

The purity or identification of the compounds were checked or made by x-ray diffraction and vibrational spectroscopy and comparison was made with literature data when available. The identification of the new complexes was further confirmed by chemical analyses.

## Results and Discussion

**Synthesis and Thermal Stability.** The complexes $MUF_7$ and $M_2UF_8$ (M = Na, K, Rb, Cs, NO, $NH_4$) were prepared as pure solids. Some attempts were made to extend this series to the Li salt without success. A new form of $NaUF_7$ (cubic) was isolated in an attempt to grow single crystals in liquid $UF_6$ at 200 °C. Unfortunately this new form was unable to be reproduced either at temperatures between 65 and 220 °C or by quenching at −196 °C. From an analogy with the data on the phase changes obtained with the other complexes, this cubic form is thought to be metastable at room temperature, whereas at higher temperature where it could be stable, the decomposition rate of $NaUF_7$ into $Na_2UF_8$ prevents its reproducible isolation. As for the "normal" form, the decomposition of cubic $NaUF_7$ is rapid at 100 °C liberating $UF_6$ and producing $Na_2UF_8$. The latter is decomposed at 300 °C to give $UF_6$ and pure NaF, with no trace of any reduced form of uranium.

Conversely, the thermal decompositions of the other $M_2UF_8$ complexes (M = K, Rb, Cs, $NH_4$) take place leaving a reduced form of uranium. As already pointed out, the ammonium salts are sometimes spontaneously reduced during their preparations and their thermal stabilities were not further studied. The stabilities of the other complexes were found to increase with

the atomic weight of the cation. $K_2UF_8$ decomposes above 300 °C, $Rb_2UF_8$ above 350 °C, and $Cs_2UF_8$ only above 400 °C. Under the conditions of decomposition for these compounds (≤450 °C) the uranium was normally found in the pentavalent state. Only in some cases at the highest of temperatures was the uranium found in the tetravalent state. The thermal decomposition products $UF_6$, $F_2$, $M_2UF_7$, and $M_3UF_8$ were produced in varying ratios depending on the temperature, pumping rate, and amount of starting material.

The study of the decomposition mechanism was restricted to the cesium salt. In this case $Cs_2UF_7$ is first produced, according to
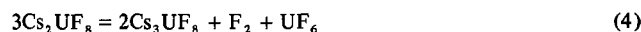
$$Cs_2UF_8 \rightarrow Cs_2UF_7 + {}^1/_2F_2 \tag{1}$$

whereas the formation of $Cs_3UF_8$ and $UF_6$ is explained through

$$3Cs_2UF_7 \rightarrow 2Cs_3UF_8 + [UF_5] \tag{2}$$

$$^1/_2F_2 + [UF_5] \rightarrow UF_6 \tag{3}$$
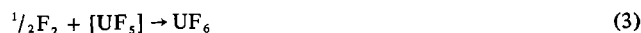
(In these equations $[UF_5]$ stands for $UF_5$ itself or its thermal decomposition residue and of course (3) has to be corrected according to the decomposition stage.)

At completion, the procedure may be written as

$$3Cs_2UF_8 = 2Cs_3UF_8 + F_2 + UF_6 \tag{4}$$

The mechanism proposed above is suggested because of the following observations: (i) With a small amount of initial solid, like that used in the microcalorimeter (∼50 mg) or in the Raman capillaries, $Cs_2UF_8$ was transformed into $Cs_2UF_7$ by heating the sample up to 450 °C in the microcalorimeter or by heating it with the high-density energy of the laser beam. In the microcalorimetry experiment $F_2$ was the only gas detected. (ii) With a larger amount of solid, on the order of a few grams, both $UF_6$ and $F_2$ were given off when the sample was heated to 450 °C in a nickel vessel in vacuo. Fluorine was the first gas given off and the solid residue was found to be $Cs_3UF_8$. The apparent discrepancy between the two results is thought to be due to the difference in the escape rate of $F_2$. With a larger amount of initial solid, this rate is slowed down by diffusion through the solid in such a way that $F_2$ is able to react with $UF_5$ to produce $UF_6$. As a result, reaction 2 can then go to completion with the formation of $Cs_3UF_8$ as the solid residue. This latter reaction has been proved by heating $Cs_2UF_7$ for 65 h in vacuo at 450 °C in a Monel reactor, which results in the formation of a few percent of $Cs_3UF_8$ and an ill-defined phase localized near the surface of the solid. From its x-ray powder pattern, this phase is attributed to $UF_x$ (4 < x < 5). These findings are consistent with the preceding observations, and the presence of fluorine in the solid is certainly necessary to drive reaction 2 to completion through the fluorination of $[UF_5]$.

**MF (M = NO, Cs), HF, $UF_6$ Systems.** These systems were studied in the hope of obtaining information on $UF_7^-$ and $UF_8^{2-}$ as pure species without the disturbing effects such as those taking place in the solid state. As previously mentioned[27] $NOUF_7$ is decomposed in pure HF but is soluble in the NOF·3HF mixture. With the addition of HF to this solution, $UF_6$ is displaced from $NOUF_7$.

These observations are consistent with the following equilibria

$$UF_7^- + HF \rightleftarrows UF_6 + HF_2^- \tag{5}$$

$$NO^+ + HF_2^- \rightleftarrows NOF + HF \tag{6}$$

These equations were also found to hold when NO was replaced by Cs. Moreover, if the concentration of MF (M = NO, Cs) is increased, the equilibria are shifted such that the number of ligands around the uranium atom is increased and

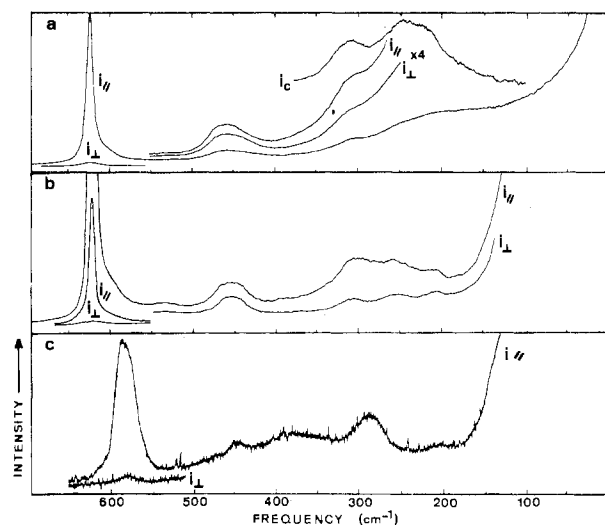**Figure 1.** Raman spectra of $UF_7^-$ and $UF_8^{2-}$ ions: (a) $NOUF_7$ in $NOF \cdot 3HF$ solution (spectral slit width 2.4 cm$^{-1}$); (b) $CsUF_7$ in CsF/HF solution (spectral slit width 2.4 cm$^{-1}$); (c) $Cs_2UF_8$ in CsF/HF solution (spectral slit width 4.8 cm$^{-1}$). $i_c$ refers to the calculated intensity (the solvent contribution is removed). $i_{||}$ and $i_\perp$ refer to the polarization directions. In (c) the band at 450 cm$^{-1}$ is mainly due to Kel-F.

the $UF_8^{2-}$ ion is formed. The identification of this latter ion in solution was made by comparison of its Raman spectrum to one obtained for the solid. The corresponding equilibrium can then be written as

$$UF_7^- + HF_2^- \rightleftarrows UF_8^{2-} + HF \qquad (7)$$

Typical Raman spectra of solutions containing the $UF_7^-$ or $UF_8^{2-}$ ions are shown in Figure 1. The corresponding frequencies are listed in Tables I and II, together with those of the solids. The bands are broad probably as a result of solute–solvent interactions and interatomic lengths and angle distributions (see discussion on solid state data). On the other hand, apart from the effect of the MF concentration on the equilibria written above, this MF concentration has an effect on both the number and the location of the bands of each species. It is convenient, for instance, to consider each species' highest stretching frequency which, in addition to being polarized, is also the most intense and best defined. For pure $UF_6$ in HF this band is found at 666 cm$^{-1}$ (the half-line width of which is 5 cm$^{-1}$ ($\Delta\bar{\nu}_{1/2}$)). Upon the addition of CsF in the molar ratio[29] of CsF:$UF_6$:HF corresponding to 8.7:0.226:100, a new band appears at 630 cm$^{-1}$, $\Delta\bar{\nu}_{1/2}$ = 25 cm$^{-1}$, which is assigned to $UF_7^-$ by comparison with a spectrum of the solid. With a further increase in the amount of CsF (e.g., CsF:$UF_6$:HF as 28.6:0.157:100) this band is shifted to 621 cm$^{-1}$ ($\Delta\bar{\nu}_{1/2}$ = 10 cm$^{-1}$) while a shoulder appears at 600 cm$^{-1}$. At higher CsF concentration the 621 cm$^{-1}$ band progressively disappears, while the shoulder is changed into a band located at 587 cm$^{-1}$ ($\Delta\bar{\nu}_{1/2}$ = 30 cm$^{-1}$). This last band is assigned to the $UF_8^{2-}$ species. In the solid samples of $UF_6$, $MUF_7$, and $M_3UF_8$, such a decrease in frequency is explained[27] by an increase of the electronic charge on the coordination sphere of the uranium atom. It is then quite reasonable to assume that such an increase in electronic charge also occurs in solution from solute–solvent interactions. The $HF_2^-$ ion, the concentration of which increases with the amount of CsF, is most likely responsible for this interaction.

The equilibria 5 and 7 written above were not studied from a quantitative point of view, but their existence is consistent with the $^{19}F$ NMR study performed on these solutions. The data reported in Table III concern the CsF/$UF_6$/HF solutions. It is seen that when $UF_6$ is absent, an increase in the CsF

concentration shifts the resonance downfield, whereas with an increase in the CsF/$UF_6$ molar ratio, this line is shifted upfield. In any case, the exchange rate was too rapid to give separate signals, thus no structural information was available from this NMR study.

Concerning this structural aspect, it may be recalled that the $UF_7^-$ ion in solution exhibits rather broad Raman bands. For the solid samples, however, the presence of five bands can be estimated from the spectra so that a pentagonal bipyramidal model may be valid for the fluorine arrangement about uranium. In the Raman spectra of solutions at higher MF concentrations, a further increase in the solute $HF_2^-$ interaction would make an anion distortion more important and would account for the appearance of the weak 535-cm$^{-1}$ Raman line, the infrared counterpart of which is strong for the solid. As far as the octafluoroanions are concerned, their spectra in solution were too poorly resolved to give any structural information. Furthermore, no infrared spectra were obtained on either the heptafluoro or octafluoro anions in solution due to experimental difficulties inherent with their corrosive natures.

**Organic Solutions.** Acetonitrile and propylene carbonate (PC) were found to be the most suitable organic solvents capable of dissolving the compounds studied here. In acetonitrile for instance, the $KUF_7$ complex was soluble and the solute/solvent molar ratio reached ~5%. The complexes $CsUF_7$ and $RbUF_7$ were less soluble and the octafluorouranates were too sparingly soluble to allow NMR or vibrational studies to be done. The vibrational data obtained from a $KUF_7$/acetonitrile solution are listed in Table I. From the number of bands observed together with their appearance in both the Raman and infrared spectra, it is clear that a $D_{5h}$ structural model is not appropriate and the spectra are closer to those observed for solid $KUF_7$. Regarding the results from the MF/HF/$UF_6$ system, a possible disturbing effect of the solvent on the actual structure of the free anion must be borne in mind. This idea is supported by the lowering of the highest U–F stretching frequency of the solute in acetonitrile when compared to the corresponding frequency found in the solid; in addition, the NMR data indicate that $UF_7^-$ is exchanging $F^-$ ions with $UF_6$ in $CH_3CN$. As mentioned below, the NMR observations are explained through extra coordination of the uranium atom by acetonitrile, giving rise to a possible disturbing effect on the surroundings of the fluorine atoms. The $^{19}F$ NMR spectra of solutions of $KUF_7$ dissolved either in PC or in acetonitrile have been recorded. In each case only one band was observed, the location of which was found to be constant in the +10 to –45 °C temperature range. In acetonitrile for a 4.5% solute/solvent molecular ratio, the chemical shift from $CFCl_3$ and the half-line width was –605.7 ppm (400 Hz) and –605.9 ppm (600 Hz) at +10 and –45 °C, respectively. These chemical shifts are consistent with the mean values observed[27] for $CsUF_7$ and $NOUF_7$ as solids, i.e., –575 and –634 ppm, respectively. The line is likely due to an exchange between the different types of fluorine atoms in $UF_7^-$, and some further experiments were made in order to understand the mechanism of this exchange. First of all, consistent with either an inter- or intramolecular exchange, the line width was found to be significantly increased with a decrease in temperature. Moreover $UF_6$, which gives a signal around –745 ppm in acetonitrile,[30] gives only one signal in the presence of $UF_7^-$ instead of two, whereas in the Raman experiment, signals for both $UF_6$ and $UF_7^-$ are observed. The NMR signal is located at –701 ppm at +10 °C for $KUF_7$/$UF_6$ at a molar ratio equal to 23.5%. At lower temperatures $UF_6$ precipitates out and the signal is shifted upfield (–672.1 ppm at –10 °C). The two species $UF_6$ and $UF_7^-$ are definitely exchanging $F^-$ ions in acetonitrile. It is worth noting that such

**Table I.** Vibrational Data[a] for NOUF₇ and CsUF₇ in CsF/HF or NOF/HF Solution, for KUF₇ in Acetonitrile Solution, and for NaUF₇, KUF₇, NH₄UF₇, and RbUF₇ in the Solid State

| NOUF₇, Raman | | CsUF₇, Raman | | KUF₇ Acetonitrile[c] soln | | KUF₇ Solid[d] | | | | | NaUF₇, solid, Raman | | | NH₄UF₇, solid, Raman | RbUF₇, Solid | | |
|---|---|---|---|---|---|---|---|---|---|---|---|---|---|---|---|---|---|
| Solid[b] | NOF, 3HF solution | Solid[b] | CsF, nHF soln | Raman | Ir | I | II | III | IV | Ir | Cub. phase | Low sym | −180 °C | | RT | −170 °C | Ir |
| 627 | 626 p | 622 | 621 p, 600 sh[e] | 620 (10) p | 617 vw | 626 | 625 | 623 | 625, 602 | 626 w | 633 (10) | 635 (10) | 636 | 625 (10) | 625 (10) | 624 (10), 593 (0.1) | 625 w |
| | | | 535[e] | 540 (0.1), 523 (0.1) | 535 vs | | 580, 541 | 544, 517, 502 | 594, 545, 520, 500, 463 | 580 sh, 540 s, br, 497 s, br | 554 (<0.1), 542 (0.1) | 554 (0.1), 541 (0.2), 515 (<0.1) | 554, 540, 516 | | 520 (<0.1) | 546 (<0.1), 517 (<0.1), 503 (0.1), 457 (0.6) | 550 s, br, 482 w, 457 m |
| | | | | | | | 496 | | | | | | | | | | |
| 446 sh, 434 | 460 dp | 462 sh, 444 | 455 dp | 454 (0.8) dp, 456 sh | 456 sh | 440 | 456, 438 | 455, 440 | 457, 441, 438 | 457 w | 450 (0.9) | 461 (0.8) | 463 | 447 (1.25) | 443 (0.9) | 442 (1) | 442 w |
| 310 | 308 p | 312 | 305 p | 312 (0.3), 294 sh | 310, 300 | 312 | 315, 300 | 311 | 313 | 438 w, 314 w, 296 sh | 310 (0.8) | 442 (0.7), 429 (0.3), 310 (1.1) | 441, 430, 312, 305 sh | 314 (0.55) | 310 (0.5) | 311 (0.7), 304 sh | |
| 240 | 245 | 249 | 250 dp | 247 (0.3) | 264, 246 | 247 | 253 | 253 | 267, 255, 248 | 256 w | 242 (1.1) | 242 (1.5) | 243 | 250 (0.76) | 248 (0.5) | 254 (0.5), 242 sh, 230 (0.3) | 230 m, 210 m |
| 210 | 215 | 211 | 210 dp | 210 (0.2) | 222 | 209 | 231, 206 | 232, 212, 201 | 232, 215, 198 | 234 s, br, 202 s, br, 140 m | 216 sh, 203 (1.2) | 215 (0.6), 204 sh | 218 | 215 (1.74), 195 (1.53) | 215 (0.4) | 207 sh, 201 (0.4) | |
| | | | | | | 80 (L), 100 }(L), 31 }(L) | | | 150, 131, 96 }(L), 32 | 100 (L) | 104, 54 }(L), 34 | 111, 91 }(L), 57, 35 | | | 100, 53 }(L), 35 | |

[a] Frequencies are given in cm⁻¹. All Raman intensities are uncorrected. Only internal or lattice (L) vibrations are listed. Unless specified, spectra were recorded at room temperature. [b] From ref 27. [c] Acetonitrile has an ir and Raman active band at 380 cm⁻¹ which is not listed here. [d] Evolution of the Raman spectrum with temperature: I, above room temperature; II, at room temperature after aging or thermal activation; III, at room temperature without thermal activation; IV, At ca. −140°. [e] Only observed for high F⁻ concentration (see text).

**Table II.** Vibrational Data[a] for the Sodium, Potassium, Nitrosyl, Ammonium, Rubidium, and Cesium Octafluorouranates

| Na$_2$UF$_8$ Raman | K$_2$UF$_8$ Raman >RT | K$_2$UF$_8$ Raman | K$_2$UF$_8$ Ir | (NO)$_2$UF$_8$ Raman −250 °C | (NO)$_2$UF$_8$ Raman | (NO)$_2$UF$_8$ Ir | NOF/HF soln[b] (Raman) | (NH$_4$)$_2$UF$_8$ Raman | Rb$_2$UF$_8$ Raman | Cs$_2$UF$_8$ Raman −200 °C | Cs$_2$UF$_8$ Raman | Cs$_2$UF$_8$ Ir | CsF/HF soln (Raman) |
|---|---|---|---|---|---|---|---|---|---|---|---|---|---|
| 607 (10) | 591 (10) | 598 (10) | 598 m | 591 (10) | 590 (10) | 590 sh | 595 p | 592 (10) | 590 (10) | 584 (10) | 583 (10) | 586 w | 587 p |
|  |  |  | 510 s, br |  |  | 534 sh |  |  |  |  |  | 578 w |  |
|  |  | 506 sh |  |  |  | 510 s |  |  |  |  |  | 508 s |  |
|  |  | 494 (0.3) |  |  |  | 498 sh |  |  | 477 (0.1) | 477 (0.3) | 474 |  | 470 |
|  | 470 (0.2) | 483 (0.3) | 460 sh | 473 (0.1) | 460 (0.1) |  |  | 470 (0.3) | 454 (0.1) | 452 (0.3) | 450 | 464 sh |  |
| 440 (0.2) |  | 463 (0.3) |  | 448 (0.2) |  |  |  | 420 (0.3) | 425 (0.1) | 418 (0.2) |  |  |  |
|  |  | 441 (0.2) |  |  |  |  |  |  |  |  |  |  |  |
| 410 (0.6) | 405 (0.5) | 408 (0.5) | 390 sh | 409 (0.4) | 407 (0.3) |  |  |  | 400 (0.4) | 398 (0.4) | 395 (0.4) |  | 390 |
| 372 (0.5) |  | 392 sh |  |  |  |  |  |  | 387 (~0.1) | 382 (0.2) |  |  |  |
| 343 (0.7) | 326 (1.5) (L) | 325 (1.5) (L) | 294 vw | 330 (1) (L) | 328 (0.9) (L) | 208 w |  | 321 (1.4) (L) | 323 (1.2) (L) | 323 (1) (L) | 321 (1.1) (L) | 270 m | 285 |
| 303 (1.1) | 292 (1.4) | 295 (1) | 260 s | 284 (1.4) | 285 (1) | 160 m |  | 286 (1.5) | 288 (1.0) | 282 (1.3) | 282 (1.1) | 176 m |  |
| 284 (1.1) |  | 286 sh | 232 s, br |  |  |  |  |  | 282 (1.0) |  |  |  |  |
| 170 (0.7) | 120 (L) | 126 (L) |  | 100 (L) |  |  |  | 112 (L) | 118 (L) | 112 (L) | 108 (L) |  |  |
| 141 (0.3) |  | 43 (L) |  | 41 (L) |  |  |  | 38 (L) | 38 (L) |  | 36 (L) |  |  |

[a] Frequencies are given in cm⁻¹. All Raman intensities are uncorrected. Only internal or lattice (L) vibrations are listed. Unless specified, spectra were recorded at room temperature. [b] Due to the bands of the solvent, the bands of the solute were not observable below ~500 cm⁻¹.

**Table III.** $^{19}$F NMR Data[a] on the CsF/UF$_6$/HF Solutions

| Molar ratio[b] | | | | $\delta$(CFCl$_3$, ext.),[c] ppm | Line width, Hz |
|---|---|---|---|---|---|
| CsF | UF$_6$ | HF | CsF/UF$_6$ | | |
| 8.7 | 0 | 100 |  | 185.6 | 52 |
| 8.7 | 0.226 | 100 | 39.5 | 166.2 | 124 |
| 28.6 | 0 | 100 |  | 167.0 | 68 |
| 28.6 | 0.157 | 100 | 18.2 | 150.9 | 840 |
| 28.6 | 0.212 | 100 | 13.5 | 144.2 | 1 050 |

[a] Temperature +10 °C. [b] See ref 29. [c] Chemical shift values as positive upfield from the CFCl$_3$ resonance.

a comparable fluoride transfer has been recently reported by Prescott et al.[31] for mixtures of WF$_6$ and TlF or CuF$_2$ in CH$_3$CN solution. In addition it has been found here that KWF$_7$, prepared by reaction between KF and WF$_6$ in SO$_2$ and identified in solution by comparison with its Raman spectrum in the solid state, was slightly soluble in both acetonitrile and PC (~2 % M) and gave a narrow resonance at −142.4 ppm (1.2 Hz) and −143.4 ppm (1.7 Hz) at +10 °C in CH$_3$CN and PC, respectively. The interesting point was the lack of $^{19}$F–$^{183}$W satellite peaks. From this point and the assumption that the coupling is not less than a few hertz (44 Hz for neat WF$_6$) it was concluded that the bonds in WF$_7^-$ are periodically broken and re-formed through some intermolecular process in CH$_3$CN and PC. Surprisingly, the exchange still takes place in the supercooled phase of PC where at −70 °C, for instance, the signal remains unique at $\delta$ −143.4 ppm (5.6 Hz). This demonstrated intermolecular exchange for the WF$_7^-$ ion may also be reasonably assumed to take place for the similar UF$_7^-$ ion. A possible way to explain this exchange is to assume that the solvent is a strong enough donor to replace a fluoride ion in the anion. This assumption is consistent with the solvation found for UF$_6$ in CH$_3$CN[30] and with the above reported exchange between UF$_6$ and UF$_7^-$ and again with the syntheses reported by Prescott et al.[31,32] Best understood in the case of acetonitrile, the equilibria responsible for the exchange could be schematically written as

$$\text{CH}_3\text{CN:} + \text{UF}_7^- \rightleftarrows [\text{CH}_3\text{CN: UF}_7^-] \rightleftarrows [\text{CH}_3\text{CN: UF}_6] + \text{F}^- \qquad (8)$$
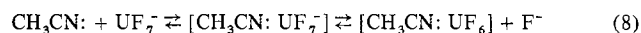
The solvation of both K$^+$ and F$^-$ is not taken into account; but these equilibria are most certainly shifted toward the left, since no band that could be attributed to UF$_6$ is seen in the Raman spectrum of this solution.

**Solid State Study.** As pointed out by Muetterties,[33] the structural determinations of the molecular geometries ought to take into account a possible nonrigid structure. Muetterties mentioned that inorganic chemistry is rich in such molecules where such dynamics take place. It is worthy to note that seven and eight coordinate species are found in this connection. One of the main observations which have been made during this study was the thermal effect on the observed vibrational spectra of the hepta- and octafluorouranates. Furthermore, that a "molecular" motion is taking place in these salts has been previously demonstrated by $^{19}$F broad line NMR spectroscopy.[34-36] Both the UF$_7^-$ and UF$_8^{2-}$ groups have been found to reorient and the ease with which they reorient increases with the increasing size of the associated cation. The reorientation motion model is not accurately known but it certainly allows an internal exchange of the fluorine atoms for which a fast exchange and relatively long time scale of observation do not allow structural determinations. This is specially true for the NMR technique for which[34-36] the difference in the shielding of the fluorine atoms of UF$_7^-$ vanishes at high temperature. On the other hand, with shorter observation time scales an instantaneous view of the motion effect is represented by disorder. Sometimes for x-ray diffraction data for instance, the resultant disorder of position or orientation of some of the atoms has to be assumed to be

averaged to account for the symmetry of the crystal field to be compatible with the symmetry of the motif. These atoms are then said to have a "statistical occupation", i.e., a partial occupation rate. In the same way this motion effect results in a larger distribution of the bond lengths and angles around the equilibrium position, giving in turn ill-defined vibrational levels. From this, both the Raman and infrared bands are then expected to be broad. The experimental data obtained on the solids are all consistent with such motion effects.

**X-Ray Diffraction Study.** Some of the structural data for the heptafluorouranates have been given previously; $CsUF_7$ has been found to exist under two forms by Sadikova et al.,[24] i.e., a cubic form at room temperature and a tetragonal form at 250 °C. On the other hand, Geichman et al.[14] have found a pseudocubic symmetry cell for $NOUF_7$ at room temperature. The diagram of $NaUF_7$ has not been indexed[18] whereas a cubic phase has been found for $KUF_7$,[26] $RbUF_7$,[26] and $NH_4UF_7$.[10] All the compounds studied here except for $NH_4UF_7$ can have two crystalline forms: a cubic and a low-symmetry form, the latter also being the lower temperature form.

The parameters of the cubic forms were found to be as follows: $KUF_7$, $a = 5.22 \pm 0.01$ Å; $RbUF_7$, $a = 5.385 \pm 0.005$ Å; $CsUF_7$, $a = 5.517 \pm 0.005$ Å; $NOUF_7$, $a = 5.334 \pm 0.007$ Å; $NH_4UF_7$, $a = 5.393 \pm 0.005$ Å; and $NaUF_7$ (fccub) ($Z = 4$), $a = 8.511 \pm 0.008$ Å. Neither the transition temperature nor the x-ray powder diagrams of the low-symmetry forms have been clearly determined, except for the cases of $NOUF_7$[28] (transition temperature) and $CsUF_7$ (transition temperature and x-ray powder diagram). The solid transition of $CsUF_7$ occurs at $15 \pm 1$ °C and its low-symmetry form x-ray diagram is indexed with a tetragonal cell, with $a = 5.30$ Å and $c = 5.37$ Å. From the noticeable shrinkage of one of the cubic axes, the decrease in volume of the unit cell reaches ca. 2.4% at the transition point.

The x-ray data of the octafluorouranates, except in the case of $Na_2UF_8$,[18] were previously unknown. The powder diagrams of the other salts were indexed with an orthorhombic cell. The corresponding x-ray data and parameters are given in Table IV. These indices were determined through comparison with isostructural complexes like $Rb_2UF_7$,[37] $K_2TaF_7$,[38] and $K_2NbF_7$[38,39] and also from the structural parentage[40] between the complexes $(NO)_2ReF_8$ and $(NO)_2WF_8$ prepared by Beaton[41] as well as from the complexes $M_2ReF_8$ (M = Rb, K) described by Ippolitov and Koz'min.[42] Since structures of both the $K_2NbF_7$ and $M_2ReF_8$ complexes have been thoroughly described, the isomorphism allowed a clear-cut indexing of the octafluorouranate patterns. It is worth adding that the data reported by Malm et al.[18] on $Na_2UF_8$, which were based on a single crystal study, have shown that this compound has a body-centered tetragonal phase; consequently it does not belong to the same structural type as the other octafluorouranates.

**Vibrational Spectroscopy.** Vibrational data obtained for the $MUF_7$ and $M_2UF_8$ complexes (M = Na, K, Rb, Cs, NO, $NH_4$) are listed in Tables I and II, respectively. The Raman spectra were found to be much more informative than the infrared spectra because the latter for the most part were broad and ill-defined. Therefore, the infrared frequencies for only some of the complexes are listed in these tables and the spectra are not shown. The temperature effect on the Raman spectra was particulary spectacular for $KUF_7$ and is displayed in Figure 2 and Table IV. For those temperatures estimated to be higher than 40 °C (cubic phase range), the Raman spectrum is closely related to those obtained for the $UF_7^-$ ion in solution and only five bands are apparent (see Figure 2, spectrum I). This type of spectrum with only minor changes has been found for all the heptafluorouranates in their cubic
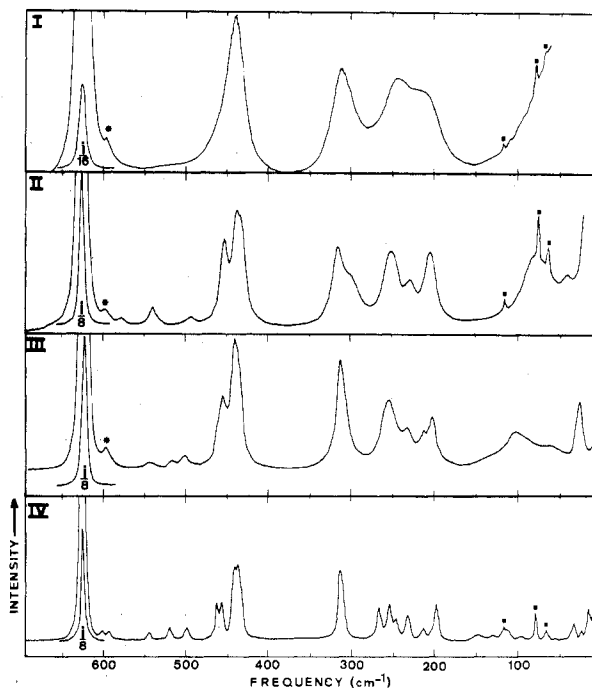


**Figure 2.** Raman spectra of solid $KUF_7$: (I) above room temperature (ca. +40 °C) (spectral slit width 3.2 $cm^{-1}$); (II) at room temperature after aging or thermal activation (spectral slit width 3.2 $cm^{-1}$); (III) at room temperature (spectral slit width 2.4 $cm^{-1}$); (IV) at ca. −140 °C (spectral slit width 2.4 $cm^{-1}$). The band with an asterisk is due to a small amount of $K_2UF_8$ and the bands with solid squares are due to the laser plasma.

phase and is thought to arise from a dynamic effect. As the motion of the fluorine atoms about uranium in $UF_7^-$ increases with temperature, the symmetry of the group increasingly averages out to pseudo-$D_{5h}$. This trend is shown up in the departure from this symmetry as the temperature decreases, which results in appearance of a shoulder on the band at 440 $cm^{-1}$ and two weak bands at 500 and 550 $cm^{-1}$.

As the temperature decreases to ~20 °C, i.e., the sample reaches the low-symmetry crystalline phase, the Raman spectrum of $KUF_7$ displays a larger number of narrower bands (spectrum III). A further change of the spectrum is obtained (spectrum II) by aging or by a weak transitory thermal activation of the solid, for instance, through a short pulse of energy from the argon ion laser tuned to 200 mW followed by return to the previous power (~20 mW). It is then thought that spectrum III is in fact representative of a metastable state of $KUF_7$, which most likely comes from a previous cooling of the solid, the stable form being that one corresponding to spectrum II. It is noticed that the infrared spectrum is closely related to the Raman spectrum II probably as a result of the beam temperature effect. On the other hand, spectrum III is related to the spectrum recorded at −138 °C (spectrum IV). Again, as no phase change has been found in this temperature range, the difference between the two spectra is attributed to a change in the molecular motion rate. This slowing down of the motion at low temperature is reversed with an increase of temperature. Spectrum II would then be representative of a thermodynamically nonequilibrated metastable state in which superfreezing of the motion is taking place. Concerning the structural point of view, it is possible that with an increase in the molecular motion rate, the equilibrium interatomic distances are spread out over a wider variety of values. As a result, small inequivalencies of the fluorine atoms are lost, creating, in general, two different sets of atoms, one set containing two atoms and the other set containing five atoms, as required for the proposed pseudo-$D_{5h}$ symmetry model. At

**Table IV.** X-Ray Data for the Potassium, Nitrosyl, Ammonium, Rubidium, and Cesium-Octafluorouranates

**$K_2UF_8$**

| d, Å | Intensity | hkl |
|---|---|---|
| 5.43 | ms | 110 |
| 5.13 | s | 021 |
| 4.60 | ms | 111 |
| 4.35 | m | 002 |
| 3.50 | w diffuse | 102 |
| 3.47 | m | 130 |
| 3.40 | m | 112 |
| 3.24 | m diffuse | 131, 040 |
| 3.015 | mw | 200 |
| 2.728 | f | 220, 132 |
| 2.653 | vw | 023 |
| 2.604 | mw diffuse | 221 |
| 2.575 | mw | (050), 042 |
| 2.492 | w | 202 |
| 2.433 | vw | 212 |
| 2.371 | w | 231 |
| 2.321 | vw | 222 |
| 2.285 | w | 151 |
| 2.241 | vw | 133 |
| 2.202 | w | 240, 052 |
| 2.156 | mw | 043 |
| 2.083 | mw | 061 |
| 2.060 | vw | 213, 024 |
| 2.000 | m | 300, 223 |
| 1.967 | m | 161, 242 |

Orthorhombic
a = 6.038 ± 0.014 Å
b = 12.899 ± 0.028 Å
c = 8.728 ± 0.022 Å

**$(NO)_2UF_8$**

| d, Å | Intensity | hkl |
|---|---|---|
| 5.46 | m | 110 |
| 5.29 | ms | 021 |
| 4.64 | m | 111 |
| 4.41 | mw | 002 |
| 3.67 | mw | 022 |
| 3.57 | m | 130 |
| 3.44 | ms | 112 |
| 3.31 | m | 040, 113 |
| 3.007 | w | 200 |
| 2.782 | w | 211, 132 |
| 2.699 | vw | 023 |
| 2.659 | vw | (050), 042 |
| 2.628 | mw | 221 |
| 2.602 | m | 113 |
| 2.490 | mw | 230, 202 |
| 2.440 | mw | 212, 150 |
| 2.352 | w | 151 |
| 2.277 | w | 222 |
| 2.236 | w | 052 |
| 2.216 | w | 240 |
| 2.161 | mw | 004, 043 |
| 2.136 | w | 232, 241 |
| 2.055 | w | 152 |
| 2.011 | mw | 114 |
| 1.997 | mw | 223, 300 |
| 1.940 | w | 250 |
| 1.883 | w | 251 |
| 1.813 | vw | 162, 134, 153 |
| 1.783 | ms | 252, 170 |
| 1.757 | m | 331 |
|  |  | 144 |

Orthorhombic
a = 6.012 ± 0.005 Å
b = 13.311 ± 0.011 Å
c = 8.861 ± 0.008 Å

**$(NH_4)_2UF_8$**

| d, Å | Intensity | hkl |
|---|---|---|
| 7.46 | w | 011 |
| 6.23 | w | 100 |
| 5.60 | s | 110 |
| 5.32 | s | 021 |
| 5.13 | vw | (101) |
| 4.80 | s | 111 |
| 4.60 | vw | 120 |
| 4.49 | mw | 002, (030) |
| 3.64 | m | 130 |
| 3.52 | mw | 112 |
| 3.36 | ms | 131, 040 |
| 3.15 | w | 200 |
| 2.928 | w | 013 |
| 2.905 | w | 211 |
| 2.820 | w | 132, 141 |
| 2.712 | mw | (103), 221 |
| 2.649 | w | 113 |
| 2.575 | w | 230 |
| 2.509 | w broad | 123, 033 |
| 2.459 | mw | 150 |
| 2.381 | w | 151 |
| 2.293 | mw | 052, 240 |
| 2.215 | w broad | 014, 241 |
| 2.161 | mw | 152, 061 |
| 2.113 | vw | 104, 143 |
| 2.065 | mw | 223 |
| 2.045 | mw | (301), 250, 242 |
| 2.012 | vw | 034 |

Orthorhombic
a = 6.305 ± 0.013 Å
b = 13.431 ± 0.023 Å
c = 9.018 ± 0.016 Å

**$Rb_2UF_8$**

| d, Å | Intensity | hkl |
|---|---|---|
| 7.52 | w | 011 |
| 6.36 | vw | 100 |
| 5.64 | m | 110 |
| 5.36 | s | 021 |
| 4.78 | m | 111 |
| 4.51 | mw | 111 |
| 4.39 | w | (030) |
| 4.10 | w | 002 |
| 4.03 | w | 121 |
| 3.63 | vs | 031 |
| 3.51 | m | 130 |
| 3.36 | ms | 112 |
| 3.167 | vw | 040, 131 |
| 2.820 | w | 122 |
| 2.688 | mw | 141, 132 |
| 2.561 | w | 023 |
| 2.460 | mw | 202 |
| 2.387 | mw | 142, 033 |
| 2.285 | vw | 151, 222 |
| 2.225 | ms | 133 |
| 2.164 | m | 232, 241 |
| 2.052 | m | 152, 014 |
| 2.034 | m | 114, 250 |
|  |  | (301), 242 |

Orthorhombic
a = 6.265 ± 0.016 Å
b = 13.479 ± 0.037 Å
c = 8.776 ± 0.021 Å

**$Cs_2UF_8$**

| d, Å | Intensity | hkl |
|---|---|---|
| 5.90 | mw | 110 |
| 5.57 | m | 021 |
| 4.96 | mw | 111 |
| 4.69 | mw | (030), 120 |
| 4.16 | mw | 031 |
| 3.78 | s | 130 |
| 3.65 | m | 112 |
| 3.50 | m | 131, 040 |
| 3.305 | mw | 122 |
| 3.217 | mw | 200 |
| 2.937 | vw | 220, 132 |
| 2.802 | vw | 221, 050 |
| 2.665 | vw | 230, 202 |
| 2.558 | w | 231 |
| 2.489 | w | 222, 151 |
| 2.313 | m | 043, 004, 232 |
| 2.260 | mw | 061 |
| 2.199 | w | 213 |
| 2.137 | ms | 161 |
| 2.125 | w broad | 250, 242, 223 |
| 1.987 | w | 153, 134 |
| 1.959 | mw | 302 |
| 1.917 | vw | 331 |
| 1.880 | mw | 243, 204 |
| 1.868 | mw | 214, 063 |
| 1.852 | mw | 144, 261 |

Orthorhombic
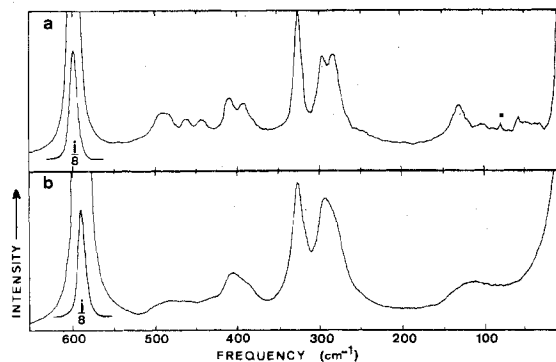a = 6.480 ± 0.010 Å
b = 14.036 ± 0.022 Å
c = 9.272 ± 0.012 Å

**Figure 3.** Raman spectra of solid $K_2UF_8$: (a) at room temperature (spectral slit width 3.2 cm$^{-1}$); (b) above room temperature (ca. +40 °C) (spectral slit width 3.2 cm$^{-1}$).

low temperature, the Raman spectrum of KUF$_7$ exhibits 21 bands, 18 of them being due to the internal vibrations. This number is in agreement with a symmetry at most equal to $C_{2v}$, since for this group 18 bands would be Raman active according to the selection rules.

In the octafluoro anion group, $K_2UF_8$ is also well representative of the marked effect of the temperature on the spectra. As seen in Figure 3, obtained at a temperature higher than room temperature (laser beam tuned to 500 mW), its Raman spectrum is very different from the spectrum obtained at, or very close to, room temperature (laser beam tuned to 5 mW). With a temperature increase, the shoulders in the bands at 295 and 408 cm$^{-1}$ and the small bands around 470 cm$^{-1}$ tend to disappear, whereas the highest frequency decreases from 598 to 591 cm$^{-1}$. The spectrum obtained at higher temperature is close to those obtained[27] for $(NO)_2UF_8$ and $Cs_2UF_8$ scanned near room temperature. It is noticed that the band seen around 325 cm$^{-1}$ in these solids has not been observed for $UF_8^{2-}$ in solution; therefore, as no other major change between the spectra of the solids and those in solution has been noticed, this band is assigned to a lattice vibration. In the same way, the bands found at ca. 100 and 40 cm$^{-1}$ (the locations of which were found to be cation dependent) are also assigned to lattice vibrations. Therefore, at high temperature only four internal vibrations remain apparent in the Raman spectrum of $K_2UF_8$. Among the possible point group symmetries which have been reported in the literature for the XY$_8$ system, it is established from group theory that 4, 6, 7, 7, 15, and 21 bands should be Raman active and 2, 7, 5, 5, 9, and 17 infrared active for the groups $O_h$, $D_{3d}$, $D_{4h}$, $D_{4d}$, $D_{2d}$, and $C_{2v}$, respectively. Coincidences should occur only in the last two groups among the 9 and 17 bands given for $D_{2d}$ and $C_{2v}$, respectively.

Therefore, as in the case for the heptafluorouranates which involved a motion effect, the Raman spectra of the octafluorouranates at high temperature look like they are due to species of a higher symmetry; that is, with only four Raman active internal vibrations, they correspond to a cubic arrangement ($O_h$ group). At lower temperatures, the molecular motions are slowed down and the Raman and infrared spectra contain 10 and 7 bands, respectively, for the internal vibrations which, with four coincidences, are consistent with a symmetry at most equal to $D_{2d}$ (dodecahedral arrangement).

## Conclusions

Apart from having given additional data on the hepta- and octafluorouranates(VI), this study has shown the marked effect of the temperature, the media, and the cation size on the apparent structure of the anions studied.

It turns out that the actual geometry of these anions is easily disturbed by the external forces that are taking place in the various media either by solvation or crystalline field forces.

The ease of distortion of these anions is most likely related to different conformations which are close to one another in energies. This effect can be paralleled to the fluorine internal exchange previously observed in the solids by NMR spectroscopy. From these findings in the solid state, UF$_7^-$ and UF$_8^{2-}$ have symmetries equal to or lower than $C_{2v}$ and $D_{2d}$, respectively, and an increase in the temperature results in an increase of the internal molecular rearrangement rate. As a consequence, each fluorine atom is occupying a less definite vibrational level which results in an apparent equivalence of some atoms giving what has been called the pseudo-$D_{5h}$ and $O_h$ symmetries.

Because of the cation's interaction, the anion becomes distorted and a significant portion of the anion's formal negative charge is localized on one of the fluorine atoms. It is worth noting that such a mechanism could account for the F$^-$ diffusion motion observed for NOUF$_7$ by NMR studies.[28] Such a diffusion motion, which has not been found for the alkali metal salts, has been assumed[28] to be due to the transient molecule NOF with the F$^-$ ion being allowed to pass from one UF$_7^-$ group to another in this manner. It should be noticed that according to our experimental data, the anion electronic cloud polarization results in a less symmetric structure for the anion associated to the smaller cations. On the other hand, the trend in the anion–cation interaction is also shown in the data concerning the relative thermal stabilities. Taking for instance the complex NaUF$_7$, for which the cation–anion interaction is expected to be the strongest, the distortion of the UF$_7^-$ ion results in a significant ionic character for one of the fluorine atoms and consequently a relatively covalent bond for the other U–F bonds. From this, UF$_6$ is able to escape at relatively low temperature leaving Na$_2UF_8$, whereas an anion–cation interaction likely also occurs in this compound in such a way that UF$_6$ is given off on heating, leaving only the alkali metal fluoride. Conversely for CsUF$_7$, the first step occurs at higher temperature than for NaUF$_7$, leaving also the octafluorouranate. But this time the alkali metal fluoride interaction taking place in this salt is too weak to balance the mean U–F bond strength and consequently the anion keeps its entity up to a temperature at which the U–F bond is broken (due to its relative weakness), fluorine is given off, and Cs$_2UF_7$ is left as a solid residue.

To summarize, this study has shown an anion–cation interaction assumption to be able to explain the main trends observed in the experimental data of the properties studied.

**Registry No.** NOUF$_7$, 59915-66-1; CsUF$_7$, 26297-22-3; KUF$_7$, 19610-56-1; NaUF$_7$, 19610-57-2; NH$_4UF_7$, 59982-81-9; RbUF$_7$, 59982-82-0; Na$_2UF_8$, 17499-61-5; K$_2UF_8$, 17499-60-4; (NO)$_2UF_8$, 59982-84-2; (NH$_4)_2UF_8$, 59992-13-1; Rb$_2UF_8$, 59982-85-3; Cs$_2UF_8$, 17476-96-9.

## References and Notes

(1) On leave from Argonne National Laboratory.
(2) O. Ruff and F. Eisner, *Ber.*, **38**, 742 (1905).
(3) O. Ruff and F. Eisner, *Ber.*, **40**, 2926 (1907).
(4) O. Ruff and A. Heinzelmann, *Z. Anorg. Allg. Chem.*, **72**, 63 (1914).
(5) H. Martin, A. Albers, and H. P. Dust, *Naturwissenschaften*, **33**, 370 (1946).
(6) Hurd, U.S. Atomic Energy Commission Report AECD 4328 (1950).
(7) H. Martin, A. Albers, and H. P. Dust, *Z. Anorg. Allg. Chem.*, **265**, 128 (1951).
(8) Worthington, Industrial Group (United Kingdom Atomic Energy Authority) Report R/CA, 200 (1957).
(9) N. S. Nikolaev and V. F. Sukhoverkhov, *Dokl. Akad. Nauk SSSR*, **136**, 621 (1961).

(10) B. Volasek, *Croat. Chem. Acta*, **33**, 181 (1961).
(11) J. R. Geichman, P. R. Ogle, and L. R. Swaney, Goodyear Atomic Corporation Report GAT-T-809 (1961).
(12) I. Sheft, H. H. Hyman, R. Adams, and J. J. Katz, *J. Am. Chem. Soc.*, **83**, 291 (1961).
(13) U.S. Patent 3 039 846 (1962).
(14) J. R. Geichman, E. A. Smith, and P. R. Ogle, *Inorg. Chem.*, **2**, 1012 (1963).
(15) S. Katz, Oak Ridge National Laboratory Report ORNL 3497 (1964).
(16) S. Katz, *Inorg. Chem.*, **3**, 1958 (1964).
(17) L. McNeese, Oak Ridge National Laboratory Report ORNL 3494 (1964).
(18) J. G. Malm, H. Selig, and S. Siegel, *Inorg. Chem.*, **5**, 130 (1966).
(19) S. Katz, *Inorg. Chem.*, **5**, 666 (1966).
(20) I. Peka, *Collect. Czech. Chem. Commun.*, **37**, 4245 (1966).
(21) I. Peka, *Collect. Czech. Chem. Commun.*, **31**, 4469 (1966).
(22) I. Peka, *Collect. Czech. Chem. Commun.*, **32**, 426 (1967).
(23) A. T. Sadikova and N. S. Nikolaev, *Atomnaia Energuia*, **25**, 422 (1968).
(24) A. T. Sadikova, G. G. Sadikov, and N. S. Nikolaev, *Atomnaia Energuia*, **26** (3), 239 (1969).
(25) G. Besnard, A. J. Dianoux, O. Hartmanshenn, H. Marquet-Ellis, and N. H. Nghi, *Commis. Energ. At. [Fr.], Rapp.*, R-3732 (1969).
(26) A. Paillet, Thesis, Lyon, France, 1972.
(27) R. Bougon, R. M. Costes, J. P. Desmoulin, J. Michel, and J. L. Person, *Inorg. Nucl. Chem. Suppl.*, 99 (1976).

(28) P. Charpin, J. Michel, and P. Rigny, *Inorg. Nucl. Chem. Suppl.*, 131 (1976).
(29) These molar ratios are relative to the initial amount of materials, and due to a possible precipitation of a solid complex, e.g., $MUF_7$ or $M_2UF_8$; the actual composition may deviate from these figures.
(30) R. Bougon, unpublished data. Since this work, we have been aware of the work of J. Berry et al. on the oxidizing and fluoride ion acceptor properties of $UF_6$ in acetonitrile which is in agreement with our findings.
(31) A. Prescott, D. W. A. Sharp, and J. M. Winfield, *J. Chem. Soc.*, Dalton *Trans.*, 934 (1975).
(32) A. Prescott, D. W. A. Sharp, and J. M. Winfield, *J. Chem. Soc.*, *Dalton Trans.*, 936 (1975).
(33) E. L. Muetterties, *Inorg. Chem.*, **4**, 769 (1965).
(34) A. J. Dianoux and P. Rigny, *J. Phys.*, **29**, 791 (1968).
(35) A. J. Dianoux, Thesis, Lyon, 1969.
(36) J. L. Person, Thesis CNAM, Paris, 1975.
(37) R. A. Penneman, G. D. Sturgeon, L. B. Asprey, and F. H. Kruze, *J. Am. Chem. Soc.*, **87**, 5803 (1965).
(38) J. L. Hoard, *J. Am. Chem. Soc.*, **61**, 1252 (1939).
(39) G. L. Brown and L. A. Walker, *Acta Crystallogr.*, **20**, 220 (1966).
(40) Pr. N. Bartlett, private communication.
(41) S. P. Beaton, Ph.D. Thesis, University of British Columbia, 1966.
(42) E. G. Ippolitov and P. A. Koz'min, *Dokl. Akad. Nauk SSSR*, **5**, 1081 (1962).

# Photoacoustic Spectroscopy of Iridium Carbonyl Halide Linear-Chain Conductors

A. ROSENCWAIG, A. P. GINSBERG,* and J. W. KOEPKE

Optical studies of polycrystalline linear-chain conductors are of considerable current interest. However, these materials are generally highly light-scattering and thus difficult to study by conventional optical transmission or reflection techniques. Photoacoustic spectroscopy offers a highly effective means for obtaining optical spectra on such materials, and we report here the first photoacoustic study of this class of materials in the 250–1000-nm range, in particular, of the compounds $K_{0.60}Ir(CO)_2Cl_2 \cdot 0.5H_2O$, $K_{0.98}Ir(CO)_2Cl_{2.42} \cdot 0.2CH_3COCH_3$, $(TTF)_{0.61}Ir(CO)_2Cl_2$ (TTF = tetrathiafulvalenium), and $Cs_{0.60}Ir(CO)_2Br_2$. These compounds contain conducting linear chains of square-planar *cis*-$[Ir(CO)_2X_2]^{0.6-}$ (X = Cl, Br) units. Their photoacoustic spectra show three absorption bands below 650 nm at 2.3, 2.9, and ~3.4 eV, which are assigned as metal-to-ligand charge-transfer transitions from the a($yz$) and b($xz$) metal orbitals to the predominantly ligand CO b($\pi^*$, $6p_z$) orbital. Above 650 nm the spectrum rises strongly toward the infrared region. This rise is the high-energy end of a broad absorption band extending from ~0.1 to 2 eV as subsequently shown by conventional infrared transmission spectroscopy. It is assigned as the transition from the $5d_{z^2}$ band to b($\pi^*$, $6p_z$). The width and energy of this transition appear to depend upon chain length, exhibiting a significant broadening and shift to higher energy upon crushing of the sample. All of the observed linear-chain transitions are considerably red-shifted with respect to the corresponding transitions in nonchain $[Ir(CO)_2Cl_2]^-$. The red shift is attributed to interactions along the chain which raise the energy of a($yz$), b($xz$), and a($z^2$) and lower the energy of b($\pi^*$, $6p_z$).

Polycrystalline linear-chain conductors are generally highly light-scattering materials that are quite difficult to study in the optical region by conventional transmission or reflection spectroscopy. Since optical spectra of these materials are of considerable interest in providing information about their electronic structure, linear-chain conductors are excellent candidates for examination by the newly developed technique of photoacoustic spectroscopy.[1-3] In this paper we describe a photoacoustic study of the recently characterized compounds[4] $K_{0.60}Ir(CO)_2Cl_2 \cdot 0.5H_2O$, $K_{0.98}Ir(CO)_2Cl_{2.42} \cdot 0.2CH_3COCH_3$, $(TTF)_{0.61}Ir(CO)_2Cl_2$ (TTF = tetrathiafulvalenium), and $Cs_{0.60}Ir(CO)_2Br_2$. These compounds all contain conducting linear chains of square-planar *cis*-$[Ir(CO)_2X_2]^{0.6-}$ (X = Cl, Br) units, as illustrated in Figure 1.

In photoacoustic spectroscopy of solids, light absorbed by a solid sample is detected as an acoustic signal. It has been possible with this technique to obtain optical absorption spectra of almost any type of material, irrespective of whether the sample is crystalline or amorphous, a powder or a gel. Since only the *absorbed* light is converted to sound, scattered light, which presents such a severe problem when dealing with many solid materials by conventional means, presents no major problem in photoacoustic spectroscopy. Our results for the

*cis*-$[Ir(CO)_2X_2]^{0.6-}$ linear chains show several notable features. In particular, we find that the linear chains have a near-ir absorption of variable frequency, apparently dependent on the chain length and not present in *cis*-$[Ir(CO)_2Cl_2]^-$ in the absence of chain formation. Also, the uv–visible region absorption of the chain complex is significantly red-shifted in comparison to nonchain $[Ir(CO)_2Cl_2]^-$, contrary to what might be expected in view of the higher Ir oxidation state in the chain complex. These effects are attributed to metal–metal interaction along the chain axis which results in band formation and raises the energy of the d levels from which the observed transitions originate.

## Experimental Section

$K_{0.60}Ir(CO)_2Cl_2 \cdot 0.5H_2O$, $K_{0.98}Ir(CO)_2Cl_{2.42} \cdot 0.2CH_3COCH_3$, $(TTF)_{0.61}Ir(CO)_2Cl_2$, and $Cs_{0.60}Ir(CO)_2Br_2$ were prepared and characterized as described previously.[4] $(C_6H_5)_4As[Ir(CO)_2Cl_2]$ was prepared by the method of Forster[5] and characterized by its ir spectrum. Photoacoustic spectra in the range 250–1000 nm were obtained as described elsewhere;[1-3] the polycrystalline powders were studied both before and after grinding in an agate mortar. The absorption spectrum of $K_{0.98}Ir(CO)_2Cl_{2.42}$ in the region 600–17 000 nm was also determined with a Cary Model 14 R spectrophotometer (600–2500 nm) and a Perkin-Elmer Model 457 IR spectrophotometer